A CRITICAL SHEAR STRAIN CRITERION FOR THE DUCTILE – BRITTLE TRANSITION IN HY100 STEEL UNDER MIXED MODE I & II LOADING

D. Bhattacharjee[1] and J.F. Knott[2]

[1] Tata Steel, Jamshedpur 831001, India
[2] School of Engineering, Institute of Metallurgy and Materials, The University of Birmingham, Edgbaston, Birmingham B15 2TT, UK.

ABSTRACT

Micromechanisms producing ductile and brittle damage operate in parallel at a crack tip. The dominant mode of failure depends upon which of the two (ductile or brittle) damage parameters first reaches its critical value. This has been shown by a study of ductile-brittle transition behaviour in HY100 steel under mixed mode I and II loading. The transition from ductile to brittle behaviour in HY100 steel was found to be affected by mixed mode I and II ratio (ratio of imposed tensile and shear loading) in a manner such that with increasing shear the transition temperature decreased. In this paper, a criterion is proposed based on the shear strain ahead of a notch tip, to predict the fracture behaviour at any given temperature and mixed mode ratio.

1 INTRODUCTION

Ductile to brittle transition in fracture behaviour with change in test temperature is exhibited by steels and other bcc metals. In steels, at low temperature the fracture is tensile stress controlled, occurring predominantly by transgranular cleavage and is associated with low energy absorption and small strains at the crack tip. It is well known that at higher temperatures, engineering materials such as steels exhibit plasticity ahead of the crack tip and the tensile stress around the crack tip decreases as the yield stress decreases. The tensile stress ahead of the crack tip may decrease to values lower than the critical stress required for initiating cleavage fracture. Crack initiation then occurs after a critical level of damage accumulation that results from crack tip blunting, void nucleation and growth. In this case, crack propagation often occurs by void linkage along a shear band, for example, in quenched and tempered HY80 [1] and HY130 [2] steels and in clean maraging steels [3]. The accumulation of shear strain contributes strongly to these processes of ductile damage and crack propagation [4] and becomes particularly important in materials with low strain hardening exponents because perturbations in the strain field occur without appreciable hardening and therefore lead to shear localisation [5, 6, 7].

The transition from brittle to ductile fracture may therefore be equated to a transition from a tensile stress controlled fracture to one that is controlled by shear strain. The ratios of imposed tension and shear are then likely to affect the transition behaviour of steels. An arbitrarily oriented crack in an engineering structure is subjected to pure tensile loading when the crack plane is exactly normal to the loading direction. At any other orientation, the crack is subjected to a mixture of modes I, II and III (i.e., mixture of tensile, in-plane shear and out-of-plane shear) loading. The commonly used criteria for ductile-brittle transition behaviour are typically based on tests carried out under mode I alone. However, from a practical point of view, it is important that a complete set of criteria for ductile-brittle transition should include behaviour under mixed mode loading.

This paper attempts to develop a ductile/brittle transition criterion based on temperature, crack tip tensile stress and crack tip shear strain that can be easily derived from the applied load and the crack plane orientation.

2 EXPERIMENTAL DESIGN

2.1 The material

The material used for the study was HY100 steel with nominal chemistry of C 0.17%, Mn 0.35%, P 0.009%, S 0.005%, Si 0.17%, Cr 1.69%, Ni 3.25% and Mo 0.40%.

Test pieces were machined to dimensions: length L=110mm, width W=20mm and breadth B=10mm. The samples were held at 950 °C for 2 hours and then water quenched. The results reported in this paper correspond to samples that were subsequently tempered at 250 °C.

Crack-like slits were introduced in the test pieces using a 0.15mm thick SiC slitting wheel taking care to maintain a/W ratio of about 0.5. Fracture behaviour with these cracks was similar to that with pre-fatigued starter cracks. Tests were carried out on a servo-hydraulic universal testing machine of 250 kN load capacity, under position control at cross displacement rate of $2\text{x}10^{-3}$ mm/sec.

2.2 Mixed Mode Tests

In this study, pure mode I crack fracture behaviour was studied under symmetric four point (S4P) bend loading while testing under mixed modes I and II was carried out using asymmetric four point bend (AS4P) specimens. The loading arrangements and the corresponding shear force and bending moment diagrams are discussed in detail by Maccagno and Knott [8] and Bhattacharjee and Knott [9]. Tests were carried out at different mixed mode ratios by varying the position of the crack (S_O) from the centre-line of the loading configuration.

For the AS4P configuration the stress intensity factors are given as:

$$K_I = 2\frac{PS_o}{W^2}\sqrt{\pi a}Y_I\,; \quad K_{II} = \frac{P}{3W}\sqrt{\pi a}Y_{II} \tag{1}$$

Y_{I} and Y_{II} are calibration factors which are functions of the crack length to specimen width (a/W ratio) and are introduced to account for the effect of finite specimen size. In this work the calibrations of Suresh et al [10] have been used.

3 DUCTILE-BRITTLE TRANSITION BEHAVIOUR

3.1 Brittle behaviour under mixed mode loading

One of the more commonly used criteria for fracture in the lower shelf region is a stress based criterion proposed by Erdogan and Sih [11]. This criterion states that crack extension starts at the crack tip in a radial direction and this radial direction is perpendicular to the direction of the greatest tension. Thus the reference is to polar coordinates with crack extension in the radial direction and stress acting perpendicular to it in the tangential direction. The stress at fracture, according to this Maximum Tangential Stress (MTS) criterion, is given by:

$$\sigma_{\theta\theta f} = \frac{K_{If}}{\sqrt{2\pi r}}\left(\cos^3\frac{\theta_o}{2}\right) - \frac{K_{IIf}}{\sqrt{2\pi r}}\left(\frac{3}{2}\cos\frac{\theta_o}{2}\sin\theta_o\right) \tag{2}$$

In the above equation $\sigma_{\theta\theta f}$ is the tangential stress at failure and θ_o is the observed fracture angle and subscript *f* for the stress intensity factors denotes values at failure.

The MTS criterion is based on linear elastic fracture mechanics. In tensile stress controlled failure, stress at fracture should not vary with mixed mode ratio as crack initiation occurs when the local tensile stress exceeds a critical tensile stress. Thus a comparison of the fracture stresses obtained at different mixed mode ratios would be a test for the tensile stress controlled mechanism.

It has been shown by Maccagno [12], Yokobori et al [12] and Bhattacharjee and Knott [13] that at -196 °C fracture behaviour under mixed mode loading indeed follows the MTS criterion.

3.2 Ductile behaviour under mixed mode loading

When tested at room temperature the mixed mode specimens did not fracture at an angle to the starter notch, but the crack propagation was instead coplanar with the starter notch, Bhattacharjee and Knott [9], irrespective of the mixed mode ratio. The initiation of such a crack is preceded by blunting of one side of the notch and shear strain localisation at the sharpened side from which the crack initiates. It has been shown [9] that initiation of such coplanar cracks occurs at a crack tip shear strain value of about 0.4. This was also supported by a dislocation model based on void initiation by decohesion at carbide particles. This model, however, does not provide a method for calculating the critical shear strain required for crack initiation in shear, from the macroscopic measured parameters of load, mixed mode ratio and temperature.

3.3 Competing damage mechanisms

It is clear that the damage mechanisms are widely different - the lower shelf being controlled by tensile stress and the upper shelf by shear strain. Earlier studies have shown that this transition in mechanism is a function of both temperature and mixed mode ratio [13]. With increasing applied Mode II component there is an increasing tendency of the crack to propagate in the coplanar or "shear" mode. Aoki et al [14] showed that a notch with a semi-circular tip deforms under mixed mode loading in a manner such that one side sharpens and the other side blunts. It was also shown that for higher Mode I component, the damaged region was at the blunted side. For a higher Mode II component, the damage region shifted to the sharpened side of the notch.

On the basis of the observations made above, it can be deduced that ahead of a crack tip, a competition exists between tensile stress controlled and shear strain controlled fracture mechanisms. Because of the geometry of mixed mode loading, the locations of maxima in shear strain and tensile stress are physically separate, thus leading to macroscopically different crack propagation directions.

Similar ductile-brittle transition behaviour is observed for Mode I loading of clean, high strength and tempered, low-alloy steels. As a result of the loading geometry, the crack growth is macroscopically in the same direction under both brittle and ductile conditions, but at the microscopic level, the ductile crack propagates in a "zig-zag" manner [15], following localised shear bands. In the following sections a criterion is developed to predict the fracture behaviour from global parameters such as test temperature and applied load.

4 MODELLING THE TRANSITION - PREDICTION USING GLOBAL PARAMETERS

4.1 Critical crack tip shear displacement

The critical crack tip shear strain at which a shear crack initiates for HY100 grade of steel has been experimentally found to be around 0.4 [9,16]. It has been shown [16] that a micromechanistic model for crack intitiation through void nucleation at carbide particles and subsequent coalescence also predicts a critical initiation shear strain of around 0.4.

However, this model is inadequate for the prediction of transition behaviour. The appropriate model should be able to predict, for given mixed mode ratios and under increasing loads, whether the maximum shear strain will reach its critical initiation value or the maximum tensile stress will reach its critical value first.

4.2 Estimation of local crack tip shear strain/displacement

As for the crack tip opening displacement (under Mode I loading), the crack tip shear displacement (under combined modes I and II loading) can be separated into its elastic component and plastic

component.

$$\delta_{II} = \delta_{II(el)} + \delta_{II(pl)} \tag{3}$$

Again, as for the plastic component of mode I opening displacement ($\delta_{I(pl)}$), the plastic component of the shear displacement ($\delta_{II(pl)}$) cannot be directly calculated from the external load. Therefore an indirect method is used to relate the plastic crack tip shear displacement to load.

Bilby, Cottrell and Swinden [17] developed an expression for crack tip shear displacement based on a model for dislocation movement ahead of the crack tip. For low values of π/τ_y ratio, and for materials following von Mises yield criterion (i.e., $\sigma_y = \sqrt{3}\tau_y$) this equation can be represent as

$$\delta_{II(el)} = \frac{\sqrt{3}K_{II}^2(1-\nu^2)}{\sigma_y E} \tag{4}$$

where σ_y is the yield stress. Since K_{II} is related to specimen geometry and load, $\delta_{II(el)}$ can be calculated for any load.

It is proposed here that when the crack tip shear displacement reaches its critical value, the corresponding elastic component also attains a critical limit. This proposition will be substantiated with experimental validation in subsequent sections of this paper. A point to note is that although the critical shear displacement is independent of mixed mode ratio, the elastic component of shear displacement depends upon the mode I/mode II ratio.

It is necessary to define the critical $\delta_{II(el)}$ values. Table 1 lists the experimentally measured critical shear displacement values. The load at initiation (P_i), at which the critical shear displacement was measured, is used to calculate K_{II} which is then used to determine $\delta_{II(el)}$. The best fit correlation between mixed mode ratio and $\delta_{II(el)}$ is described by the equation:

$$\delta_{II(el)}^{crit} = 0.0537 - 0.0004\arctan(K_I/K_{II}) \tag{5}$$

If the $\delta_{II(el)}$ value, calculated from Eq (4), at any given load lies on or above the solid line given by Eq (5), then fracture is predicted to be shear strain controlled.

Table 1: Values of critical elastic shear displacement obtained at room temperature.

S_o (mm)	P_i (kN) (load corresponding to γ_i)	K_I/K_{II}	K_{II} (MPa$\sqrt{m}$)	γ_i (critical shear strain at crack initiation)	$\delta_{II(el)}^{crit}$ (mm)
7.0	150.5	2.20	59.07	0.42	0.027
5.0	167.0	1.57	67.40	0.39	0.032
5.0	172.5	1.57	69.60	0.40	0.034
3.0	181.5	0.94	72.35	0.38	0.038
3.0	176.0	0.94	70.96	0.37	0.034
2.0	187.5	0.63	73.94	0.41	0.042

Note: Results obtained at room temperature. Yield stress=1050 MPa.

4.3 Effect of temperature

The values of $\delta_{II(el)}^{crit}$ vary with mixed mode ratio and temperature (as yield stress is temperature dependant). The exact relationship is developed elsewhere, Bhattacharjee and Knott [18]. The results of the analysis are shown in Figure 1. The solid lines in Figure 1 represent the best fit trends and are used for determining the values of $\delta_{II(el)}^{crit}$ at different mixed mode ratios and temperatures.

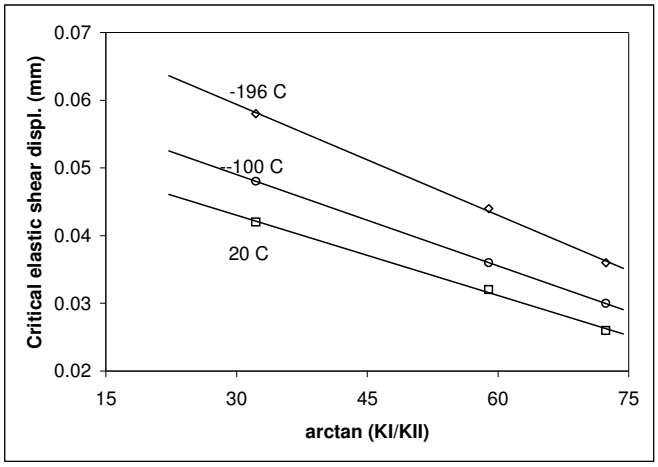

Figure 1: Variation of critical elastic shear displacement with mixed mode ration and temperature.

5 VALIDATION OF THE CRITICAL SHEAR DISPLACEMENT CRITERION

The analysis developed in the previous section results in straight lines that represent the limits defined by the values of $\delta_{II(el)}^{crit}$. For any specimen, the value of $\delta_{II(el)}$ (from Eq (4)) must reach the value corresponding to the line in Figure 1 in order for $\delta_{II(pl)}$ to attain the critical value for shear-controlled fracture.

Table 2 lists the $\delta_{II(el)}$ values for specimens tested at various temperatures and under different mixed mode ratios. For specimens that failed in tension, the load at failure, P_f, was used for the analysis, and for specimens that failed in shear, the load at initiation, P_i, was used. The comments in the "Prediction" column specify the failure mechanism as predicted by the comparison of $\delta_{II(el)}$ values with the value of $\delta_{II(el)}^{crit}$. "Shear" indicates shear failure, through a shear band, as exhibited above the transition temperature and is predicted if $\delta_{II(el)} \geq \delta_{II(el)}^{crit}$. "Tension" indicates failure below the transition temperature and is predicted if $\delta_{II(el)} < \delta_{II(el)}^{crit}$. The last column in Table 2 lists the observed fracture angles that are also indicative of the observed fracture mechanism. An angle of 0° indicates that shear fracture is observed. A non-zero fracture angle indicates that tensile-stress controlled (MTS) fracture behaviour is observed.

Since under mixed mode loading tensile stress controlled cracks propagate at an angle to the starter crack or notch and a crack growing through a shear band propagates nearly coplanar with the starter crack, it is evident from Table 3 that the predictions match well with the observations.

6 CONCLUSIONS

Different micromechanisms control crack initiation and propagation behaviour in the ductile and brittle fracture regimes. The two mechanisms of crack initiation act in parallel and therefore compete with each other. A single fracture criterion is insufficient to describe crack initiation behaviour in or near the ductile-brittle transition region. In the ductile regime crack behaviour can be described by a criterion based on critical shear displacement. A model has been developed to

enable determination of critical shear displacement from applied load, the mixed-mode ratio and ambient temperature.

Table 2: $\delta_{II(el)}$ values for specimens tested at various temperatures and different mixed mode ratios.

Temp °C	S_o (mm)	K_I/K_{II}	P_f (or P_i) (kN)	K_{II} MPa√m	σ_y (Mpa)	$\delta_{II(el)}$ (mm) [Eq (4)]	$\delta_{II(el)}^{crit}$ (mm) [Fig 1]	Prediction	Crack propgn dirn.
-196	7	2.84	73.5	41.67	1450	0.010	0.037	Tensile	31.5
	5	1.95	87.5	46.39	1450	0.012	0.042	Tensile	35.0
	2	0.78	124.0	69.95	1450	0.027	0.055	Tensile	58.0
	1	0.4	127.0	72.54	1450	0.029	0.064	Tensile	60.5
-100	10	3.15	125.2	49.63	1200	0.016	0.028	Tensile	41.0
	7	2.20	158.3	62.76	1200	0.025	0.031	Tensile	46.5
	5	1.66	178.2	70.56	1200	0.032	0.034	Tensile	55.0
	2	0.63	233.6	92.61	1200	0.056	0.047	Shear	0
-80	10	3.15	118.2	46.85	1155	0.015	0.027	Tensile	44.0
	7	2.20	156.5	62.04	1155	0.026	0.030	Tensile	52.5
	5	1.66	185.6	73.56	1155	0.037	0.033	Shear	0
	2	0.63	216.5	85.83	1155	0.050	0.045	Shear	0
20	10	3.15	137.5	54.39	1050	0.025	0.025	Shear	0
	7	2.20	153.5	60.85	1050	0.028	0.027	Shear	0
	5	1.66	178.8	70.88	1050	0.038	0.030	Shear	0
	2	0.63	192.3	76.24	1050	0.044	0.041	Shear	0

REFERENCES

1. Clayton JQ. Knott JF. Met. Sci. 1976; 10: 63-71.
2. Slatcher S. Knott JF. In: D. Francois, editor. Proc. Conf. ICF 5, Cannes, 1981; 1: 201-207.
3. Beachem CD. Yoder GR. Metall. Trans. 1973; 4: 1145-1153.
4. McClintock FA. Kaplan SM. Berg CA. Int. J. Fract. Mech. 1966; 2: 614-627.
5. Cowie JG. Tuler FR. Mater Sc. Engng. 1987; 95: 93-99.
6. Russo VJ. Chakrabarti AK. Spretnak JW. Metall. Trans. 1977; 18A: 729-740.
7. Fleck NA. Hutchinson JW. Tvergaard V. (1989) J. Mech. Phys. Solids.1989; 37: 515-540.
8. Maccagno TM. Knott JF. Engng Fracture Mech. 1989; 34: 65-86.
9. Bhattacharjee D. Knott JF. Acta Metall. et Mater. 1994; 42: 1747-1754.
10. Suresh S. Shih CF. Morrone A. O'Dowd NP. J. Am. Ceram. Soc. 1990; 73: 1257-1267.
11. Erdogan F. Sih GC. Trans. ASME, J. Basic Engng. 1963; 85: 519-527.
12. Yokobori T. Yokobori Jr, AT. Sato K. Omotami M. Engng Fracture Mech. 1983; 17: 75-85.
13. BhattacharjeeD. Knott JF. In: Miller KJ, Rossmanith P, editors. Mixed Mode Fatigue and Fracture, ESIS
14. Mechanical Engineering Publ., London, 1993; p 99-109.
14. Aoki S. Kishimoto K. Yishida T. Sakata M. J. Mech. Phys. Sol. 1987; 35: 431-455.
15. Knott JF. Met. Sci. 1980; 15: 327-336.
16. Maccagno TM. Knott JF. Engng Fracture Mech. 1992; 41: 805-820.
17. Knott JF. Fundamentals of Fracture Mechanics, Butterworths. 1973; p150-164.
18 Bhattacharjee D. Knott JF., submitted to Engng Fracture Mech.